An Ultrasonic Measurement for In-vitro Depth-dependent Equilibrium Strains of Articular Cartilage in Compression

Y. P. Zheng [1], A. F. T. Mak [1], K.P. Lau [1], and L. Qin [2]

[1] Jockey Club Rehabilitation Engineering Center, The Hong Kong Polytechnic University, Kowloon, Hong Kong SAR, China

[2] Department of Orthopaedics and Traumatology, The Chinese University of Hong Kong, N.T., Hong Kong SAR, China

Short Title: **Ultrasonic Measurement of Cartilage in Compression**

Address for correspondence:

Dr. Yongping Zheng

Assistant Professor

Rehabilitation Engineering Center

The Hong Kong Polytechnic University

Hung Hom, Kowloon

Hong Kong

Tel: (852) 2766-7664

Fax: (852) 2362-4365

Email: rczheng@polyu.edu.hk

==========

Submit to:

Physics in Medicine and Biology

First Submitted in May 08, 2002

An Ultrasonic Measurement for In-vitro Depth-dependent Equilibrium Strains of Articular Cartilage in Compression

Abstract

The equilibrium depth-dependent biomechanical properties of articular cartilage were measured using an ultrasound-compression method. Ten cylindrical bovine patella cartilage-bone specimens were tested in compression followed by a period of force-relaxation. A 50MHz focused ultrasound beam was transmitted into the cartilage specimen through a remaining bone layer and a small hole at the center of a specimen platform. The ultrasound echoes reflected or scattered within the articular cartilage were collected using the same transducer. The displacements of the tissues at different depths of the articular cartilage were derived from the ultrasound echo signals recorded during the compression and the subsequent force-relaxation. For two steps of 0.1mm compression, the average strain at the superficial 0.2 mm thick layer (0.35 ± 0.09) was significantly ($p < 0.05$) larger than that at the subsequent 0.2 mm thick layer (0.05 ± 0.07) in and those at deeper layers (0.01 ± 0.02). It was demonstrated that the compressive biomechanical properties of cartilage was highly depth-dependent. The results suggested that the ultrasound-compression method could be a useful tool for the study of the depth-dependent biomechanical properties of articular cartilage.

Keywords: articular cartilage; biomechanics; elastography; osteoarthritis; ultrasound

1. Introduction

Articular cartilage (AC) is a biological weight-bearing tissue covering the ends of articulating bones within synovial joints. Functionally, AC plays essential roles in joint lubrication and in load transmission across joints (Kempson 1980; Mow et al. 1991). Structurally, the organic composite matrix of AC can be regarded as a proteoglycan gel reinforced by a network of fine collagen fibrils and swollen with a multi-ionic electrolytic aqueous solution (Mow et al. 1991, Mankin et al. 1994). Because of the spatial variations of the water content, the proteoglycan concentration, and the orientation of the collagen fibrils, the mechanical properties of the AC are different at different depths (Mow et al. 1991, Mankin et al. 1994). To measure the depth-dependent properties of AC is important not only for the investigation of AC structure but also for the study of AC degenerations such as osteoarthritis as well as for AC tissue engineering. Experimental studies for evaluating the compressive properties of AC have conventionally relied on controlling or measuring the surface displacement or load of tissue specimens (e.g., Mow et al. 1980). However, the spatially varying compressive properties of AC could not be directly measured with such experimental approaches.

The zonal variations of the tensile properties of AC have been measured using carefully excised tissue slides (Woo et al. 1976; Roth and Mow 1980; Drogendijk and Mow 1982; Guilak et al. 1994). Confined compression tests were carried out on specimens with and without the superficial zone to assess the influence of the superficial zone on the biomechanical properties of AC under compressive loading (Setton et al. 1993). Chen et al. (2001) measured the depth-dependent mechanical properties of AC by performing confined tests on three discrete layers separated from full-thickness AC at different depths. It should be noted that the overall integrity of the cartilage tissues could not be protected during these measurements. Theoretical predictions of the nonhomogeneous deformation field within an AC layer as a concomitant result of interstitial fluid movement are also available in the literature

(Mow et al. 1980; Wang et al. 2001). However, these models are difficult to verify because of the lack of a direct measurement method for the nonuniform deformation of AC. Recently, Korhonen et al. (2002) used indentation test, quantitative polarized light microcopy, and finite element analysis to demonstrate the importance of the superficial tissue layer of AC to the indentation stiffness.

Optical methods have been used for the measurement of inhomogeneous equilibrium strains within AC during compression tests (Guilak et al. 1995, Schinagl et al. 1996, 1997). Guilak et al. (1995) studied the chondrocyte deformation and the local tissue strain in AC under compression using a confocal microscope. Schinagl et al. (1996, 1997) reported a video microscopic method to quantitate the depth-dependent strains within AC during a confined compression. In their method, fluorescently labeled chondrocyte nuclei were selected as intrinsic markers. It has been demonstrated that the strain distribution of AC in compression was significantly depth-dependent. In the optical measurement methods, the strain fields of AC were measured along one side of the excised slide of AC. It is not clear whether the depth-dependent material properties of AC obtained in such a ‘destructive’ way would be the same as those in its natural intact state.

Ultrasound can be used to characterize AC through the measurement of acoustical parameters including ultrasound speed, attenuation, spectrum, reflection coefficient, etc. Recently, ultrasound has been used to facilitate the direct measurement of overall and depth-dependent mechanical properties of AC tissues associated with a compression or indentation. Suh et al. (2001) reported a method to simultaneously measure the ultrasound speed and thickness of AC tissues by applying an indentation on the AC surface. The flight-times of ultrasound signals transmitting through an entire AC layer were measured before and after the externally measured deformation was applied to the AC. The deformed thickness of the AC was used to calculate the average ultrasound speed of the whole AC layer. Fortin et al. (2000) used 50MHz ultrasound to measure the transient lateral displacements of AC tissues at different depths under an axial compression with two flat plates. The dimensions of the specimen were in the

order of 1mm. It was demonstrated that the transient depth-dependent Poisson's ratio could be measured using this method. The strains of the AC tissues along the loading direction have not been measured in this study. It seems that the experimental setup for loading an AC specimen and meanwhile collecting high-frequency ultrasound signals along the same direction remains a challenge. Cohn et al. (1997a, 1997b) extended the elastography technique (Ophir et al. 1991, 1999) to the high-frequency ultrasound and developed an elastic microscope system. In this system, an ultrasound beam was passed through a slit (2.6mm in width) in a tissue compressor. When the tissue was compressed, it would be squeezed into the slit. By monitoring the squeezing movement of tissues at different depth of the specimen, the strain image was derived. It is obvious that the slit in this system introduced uncertainties in the mechanical boundary conditions of the specimen when used for biomechanical studies for AC. Recently, Konofagou et al. (2001) reported a computational method to simulate the elastography of poroelastic material such as AC during a compression test. Using homogeneous material properties, it was analytically demonstrated that ultrasound could be used to map sequential axial and lateral strains during the stress-relaxation phase.

Zheng and Mak (1996, 1999a, 1999b) developed a tissue ultrasound palpation system for the biomechanical assessment of skin and subcutaneous tissues using a probe with an in-series ultrasound transducer and a load sensor. By increasing the ultrasound frequency, they developed ultrasound-compression systems for the AC assessment (Zheng et al. 1998, 2001). These systems aimed to collect high-frequency ultrasound signals in the direction of the applied compression. The zonal equilibrium compressive properties of trypsin-treated AC have been successfully measured (Zheng et al. 2001). A 50 MHz contact ultrasound transducer with a silica delay line at the tip was used as a compressor to test trypsin-digested AC specimens. Distinct ultrasound reflection signals could be obtained from the interface between digested and the undigested portions of the AC specimens. Using this method, the compression moduli of the digested and undigested portions of AC were measured. However, it was difficult to differentiate the ultrasound signals scattered by other internal interfaces of the AC

using that system. The purpose of this paper was to report the depth-dependent equilibrium strains of AC under compression obtained by using a newly designed ultrasound-compression system.

2. Materials and Methods

2.1 Specimen Preparation

Fresh mature bovine patellae without obvious lesions were obtained within six hours of slaughter and stored at $-20^{\circ}C$ until experiments. Before the ultrasound-compression tests, the patella was first thawed in normal saline solution (0.15M NaCl) at room temperature (approximately $20^{\circ}C$) for one hour. The lateral part of the patella was excised using a metal saw. It was then further cut into two pieces perpendicular to the articulating surface. An AC slab with a bone layer approximately 5 mm thick was prepared from each piece. Osteochondral cylinders were then cored out from the flat area of each AC-bone slab using a metal punch with a diameter of 6.35 mm (1/4 inch). An AC specimen with a bone layer approximately 0.1~0.2 mm thick was prepared from the cylinders using a lower speed diamond saw. In comparison with the average thickness approximately 1.5 mm of the AC used in this study, this bone layer was quite thin. The reason for leaving this thin layer of bone was to maintain the integrity of AC tissues and to prevent the soft cartilage tissue from being squeezed into the hole in the specimen platform during the compression test. The small hole was used to transmit an ultrasound beam into the AC specimen; this will be explained in detail later. One AC disk was selected from each patella and used for the ultrasound-compression test. A total of 10 AC specimens were tested in this study. The AC specimens were stored at $-20^{\circ}C$ until the ultrasound-compression test. Histological studies were performed for the AC specimens after the compression test (Qin et al. 2002). Figure 1a shows a typical histological image of the central portion of an AC specimen with a Safranin-O stain. The ultrasound echo signals obtained from a cartilage specimen using the ultrasound-compression system was illustrated in Figure 1b to represent their correspondence.

2.2 Ultrasound-Compression System

Figure 2 shows the schematic diagram of the ultrasound-compression testing system used in this study. During the experiment, the container was filled with saline solution. The specimen platform was located in the middle of the container and used to carry the AC specimen. A focused ultrasound beam was transmitted into the AC specimen through a small hole in the center of the specimen platform. The diameter of the hole was approximately 0.5 mm.

A porous compressor made of compacted stainless steel mesh was used to deform the AC from the top of the specimen platform. The diameter of the compressor was 7.5 mm, and the diameter of the mesh fiber was approximately 0.05 mm. The porous compressor was formed under a pressure of approximately 300 MPa. It was assumed that the compressor was rigid during the compression test on cartilage specimens. The reason for using a porous compressor was to allow interstitial fluid movement through the AC surface during the compression and subsequent force-relaxation. Thus, a shorter relaxation time (350 s as used in this study) for reaching a state of equilibrium could be achieved. Impermeable compressors could also be used in future studies. The movement of the compressor was manually driven, with a micrometer adjustor installed on the top of the testing device as shown in Figure 2. The compressor was connected in series to a 25 N load cell (Model ELFS-T3E-5L from Entran, NJ, USA). The amplified load signal was digitized by an A/D card (Model PCL-711B from Advantech Co. Ltd., Taiwan) installed in a Pentium 200MHz PC.

A 50 MHz focused broadband polymer (PVDF) ultrasound transducer (Panametrics, Waltham, MA, USA) with a focal length of 12.7 mm was used to transmit ultrasound pulses into the AC via the saline solution and to receive the ultrasound echoes reflected or scattered within the AC. The central frequency of this transducer was 35 MHz, and its 6 dB bandwidth was 22 MHz. The 6 dB focal zone was 0.08 mm in diameter and 0.95 mm in length. The focus point of the transducer was placed approximately at the central portion of the specimen thickness by moving the

transducer to maximize the ultrasound signals from the middle portion of the AC layer. A broadband ultrasound pulser/receiver (Model 5601A from Panametrics, Waltham, MA, USA) was used to drive the ultrasound transducer and to amplify the received ultrasound echoes. The receiver bandwidth was set to 5 MHz to 75MHz. There was no time-gain-compensation function in this device. To obtain sufficient amplitude of the ultrasound scattering echoes from AC, the maximum power and amplification of the pulser/receiver were used in this study. The ultrasound reflection signals were digitized by an A/D converter card with a sampling rate of 500 MHz (Model CompuScope 8500PCI from Gage, Canada) installed in the computer. The A/D converter was triggered by the transmitting trigger of the ultrasound pulser/receiver. Since this trigger was not synchronized with the clock of the A/D converter card, there was a maximum jitter of 2 ns among the digitized echo trains.

A custom-developed computer program was used to collect the load signals and ultrasonic signals digitized by the A/D converter cards. This software was also used for the digital processing of ultrasonic signals. To improve the ultrasonic signal condition for later cross-correlation algorithm, the ultrasound echo trains were averaged 10 times to enhance the signal-to-noise ratio. With this averaging process, the effects of the jitter between the transmitting trigger of the ultrasound pulser/receiver and the clock of the A/D converter could also be reduced.

As shown in Figure 2, the bottom of the specimen platform was designed in a conical shape and covered by a layer of rubber serving as an acoustic absorber. The purpose of these designs was to allow the ultrasound beam to effectively pass through the central hole and meanwhile to reduce the reflecting echoes of the ultrasound beam at the bottom of the specimen platform. With this design, the bottom reflection was significantly reduced.

2.3 Ultrasound-Compression Test

The AC specimen was first thawed in a normal saline solution for one hour at room

temperature of approximately $20^{\circ}C$. The tests were performed with the AC disk placed at the center of the specimen platform and with the AC surface facing the compressor. The test chamber was filled with saline solution. Before the ultrasound-compression test, the compressor was gradually moved down to make contact with the specimen platform. The ultrasound echo obtained at this position was recorded as a reference. The ultrasound signal was transmitted into the AC through the hole in the specimen platform and through the thin layer of bone.

It was observed that the excised specimens were slightly curled, with the AC surface being slightly convex. During a test, the compressor was first gradually moved against the articular surface of the AC to generate a contact. The movement of the compressor was monitored with the ultrasound signal reflected from the surface of the compressor. After a contact was made between the AC and the compressor, the compressor was further driven so that the specimen could make full contact with the specimen platform. This was monitored by tracking the front of the ultrasound signal reflected from the interface of the saline solution and the bone. The compressor was manually driven and the compression rate was manually controlled, with the visual feedback from the movement of the AC surface calculated from the shift of the ultrasound echo and displayed on a computer screen. Figure 3 shows the actual movement of the AC surface as detected by ultrasound when a compression rate of approximately 0.2 mm/min was attempted manually. The mean compression rate and its standard deviation were calculated using the data from 10 tests on different specimens. The limited variations of the compression rate would not be critical in this study as only the equilibrium properties of the AC were measured. Before data recording, a pre-deformation of 0.1 mm was made at a rate of approximately 0.2 mm/min after contact conditions were achieved. After this compression, a force-relaxation period of 350 s was allowed. This reference state was defined as the initial state for the subsequent compression tests. The ultrasound-compression test of each AC specimen was performed with a two-step compression-relaxation procedure on top of the 0.1 mm pre-deformation. Each 0.1 mm compression was carried out at a

compression rate of approximately 0.2 mm/min, as described above. After each incremental compression, a force-relaxation period of 350 s was allowed. This type of compression-relaxation regimen has been commonly used for the biomechanical testing of AC (Mow et al. 1980), and it enables the equilibrium material properties of AC to be measured. Figure 4 shows the typical force-relaxation behavior of an AC disk specimen in response to the two steps of compression.

The received ultrasound signals were comprised of echoes from the saline solution/bone interface, other acoustic interfaces inside the bone, the bone/AC interface, other acoustic interfaces inside the AC, the interface between the AC surface and the saline solution, and the interface between the saline solution and the compressor surface. A complete ultrasound echo train obtained from a specimen was shown in Figure 2a. Figure 5 shows the ultrasound echoes scattered from the tissues inside the AC at different states during the compression test.

To test the repeatability of the measurement, three out of the ten AC specimen were randomly selected and measured twice. The testing protocol for each test was the same as that introduced above. After the first test, the specimen was removed from the specimen platform and submerged in a saline solution for recovery for at least two hours.

2.4 Calculation of the displacement distribution

From the ultrasound echoes as shown in Figure 5, the flight-time T of the ultrasound signal transmitted from the bone-AC interface to the AC surface and back to the bone-AC interface can be obtained. If the average ultrasound speed in the AC specimen was c, the thickness h of the entire AC layer could be calculated using the equation:

$$h = c*T/2$$

In this study, an average ultrasound speed of 1660 m/s was assumed for the AC layers. This value corresponds to a mean speed estimated in vitro in normal bovine cartilages

(Joiner et al. 2001). If the whole AC layer was devided into sub-layers, the thickness of each sub-layer could also be calculated. The effects of ultrasound speed and its zonal variation will be discussed later.

In this study, the displacement of each layer of AC during compression was derived using a cross-correlation echo tracking method. The cross-correlation method has been used for the ultrasound elastography of soft tissues (Ophir et al. 1991). In this study, it was used for tracking the movements of the selected tissue portions at different depths within the AC layer when a deformation was applied on the surface (Zheng et al. 2001).

The average portion of the superficial layer was about 10-20% of the entire AC layer (Mow et al. 1991). As the average thickness of the AC specimens used in this study was approximately 1.5 mm, the superficial layer was approximately 0.15 to 0.3 mm thick. The thickness of each sub-layer for ultrasound analysis was selected to be approximately 0.2 mm. The ultrasound echoes scattered within each sub-layer were used to measure the displacement of that sub-layer after each step of compression as shown in Figures 5a, 5b, and 5c, using the cross-correlation tracking method. The bone-AC interface was used as a reference in the calculation of the displacement. The ultrasound echo trains were recorded continuously with an interval of approximately 10 s during the compression and stress-relaxation. The movements of the selected echoes were continuously tracked in the off-line signal processing, and the displacements of the corresponding tissue layers were accumulated. Such an accumulation technique has been commonly used in the ultrasound elastography (Ophir et al. 1999). Figure 6 shows the depth-dependent displacements of tissues of a typical AC specimen at different time points. The software we developed allowed us to manually select any part of the ultrasound signals with any length of a tracking window within a sub-layer for the cross-correlation tracking. The window width used in this study ranged from a half to three cycles of the ultrasound radio frequency signals. For different specimens, the conditions of the ultrasound echoes signals were different. In some cases, the ultrasound signals within some sub-layers could be too small to be detected. In such a situation, the displacement information of that sub-layer might be missed. For the same

reason, the thickness of the selected sub-layers might not be exactly 0.2 mm. The displacement at each depth with a 0.2 mm interval was interpolated using the two neighboring data points. The average strain of each sub-layer (0.2 mm thick) was then calculated using the two interpolated data points adjacent to this sub-layer. The resolution for the flight-time measurement was 2 ns in this study, with a 500 MHz A/D converting rate. Using the assumed average ultrasound velocity of 1660 m/s for AC, the corresponding displacement resolution in AC could be up to approximately 1.7 μm.

3. Results

Figures 7a to 7f shows the equilibrium displacement distributions of three typical AC specimens throughout the depth after two increments of 0.1 mm deformation were applied and the corresponding equilibrium states were reached. The horizontal axis represents the depth from the AC surface. The results demonstrated that the displacement distributions were quite repeatable for the three randomly selected AC specimens, though the positions of the measurement points were slightly different for the two tests for each specimen. The main reason for the different measurement point was the difference of ultrasound echoes in each test, as the specimen could not be placed at the exact same location during the two tests. It was also noted in Figure 7 that the displacement distribution of AC in compression was depth-dependent, and that the dependence was non-linear. The superficial layer incurred most of the deformation applied to the AC specimen, though large variations existed among the results of individual specimens. Similar results were obtained for the other specimens.

Figure 8 shows the equilibrium strains of sub-layers at different depths of AC after two incremental compressions were applied. The mean strains and their standard deviation were calculated using the results of the 10 specimens. For the two steps of 0.1mm compression, the average strain at the superficial 0.2 mm thick layer (0.35 ± 0.09) was significantly ($p < 0.05$ for t-test) larger than that at the subsequent 0.2 mm

thick layer (0.05 ± 0.07) and those at deeper layers (0.01 ± 0.02). It was also demonstrated by the t-test that the equilibrium strain at the second 0.2 mm thick layer from the cartilage surface was significantly ($p < 0.05$) larger than that at the deeper layers for the second step of compression. There was no significant ($p > 0.05$) difference between the results of the 1^{st} an 2^{nd} compression for each corresponding layers.

4. Discussion

An ultrasound-compression testing device for assessment of the depth-dependent biomechanical properties of AC was introduced in this paper. Disk specimens of bovine patella AC with a thin layer of bone were tested using this device, and some preliminary results were reported. The device allowed the collection of ultrasound echoes scattered inside the AC, while compressing the AC specimens on their surfaces. A 50 MHz focused ultrasound transducer (with a central frequency of 35 MHz) was used in this study. A cross-correlation method was used to track the ultrasound echoes and to derive the displacement of the AC layer in the different depths. Preliminary results demonstrated that the strain distribution was rather inhomogeneous throughout the depth of the AC layer under compression. It was noted that the superficial layer incurred most of the deformation applied on the AC, while the strains in the middle zones were relatively much smaller. The results of t-test demonstrated that the equilibrium strain at the superficial zone (0.2 mm thick) was significantly ($p < 0.05$) larger than those at the deep zones. These findings were similar to those reported using optical microscopic methods. While bovine patellar AC was measured in this study, this ultrasound-compression method could also be used for the nondestructive characterization of AC from other locations and other species like human (Joiner et al 2001) and rat (Cherin et al. 2001). To facilitate further investigations of this new application of ultrasound elastography for the AC assessment, a number of issues were discussed as follow including ultrasound speed and thickness measurement, ultrasound

echoes, measurement resolutions, boundary conditions, depth-dependent deformations, and transient measurement.

4.1 Ultrasound Speed and Thickness Measurement

Many investigators have reported the ultrasound speed of the AC of different joints, of different species and in different conditions (Modest 1989, Agemura et al. 1990, Myers et al. 1995, Cherin et al. 1998, Toyras et al. 1999, Suh et al. 2001, Joiner et al. 2001). In this study, a constant ultrasound speed of 1660 m/s was assumed for all the bovine AC specimens throughout the depth (Joiner et al. 2001). Agemura et al. (1990) reported that the ultrasound speed of steer patella AC increased by approximately 5% from the superficial layer to the deep layer. The feasibility of using ultrasound for the measurement of the AC thickness has been discussed recently (Mann et al. 1999, 2001). The main concern was that the ultrasound speed of the AC was not a constant. The variation of the ultrasound speed of AC at different depths, at different locations, of different species, and under different pressures deserved to be further investigated. This issue should also be considered when the method introduced in this paper is used to study the material properties of degenerated AC. Some earlier studies had demonstrated the significant difference of ultrasound speed in proteoglycan-depleted and in intact AC (Myers et al. 1995; Suh et al. 2001, Joiner et al. 2001), but some studies had not (Agemura et al. 1990; Toyras et al. 1999).

The difference of the ultrasound speed of the AC will affect the calculation of thickness and displacement of the entire layer as well as the sub-layers. However, for the strain calculation in the compression test, the ultrasound speed can be cancelled out if it is assumed not to be a function of strains. Thus, calculation of the strain distribution will not be affected by the zonal difference in ultrasound speed when each sub-layer incurs a small local strain (Zheng et al. 2001). However, for a large local strain (over 0.35) in the superficial layer, as demonstrated in this study, the strain dependence of the ultrasound speed needs to be considered in future studies.

4.2 Ultrasound Echoes

In this study, the focused ultrasound beam was passed through a small hole with a diameter of approximately 0.5 mm located at the center of the specimen platform. Ultrasound signals were transmitted first through a thin layer of bone and then into the AC layer. The 50 MHz ultrasound attenuated significantly after passing though the bone layer, though the maximum energy and gain of the pulser/receiver were used and averaging was performed to enhance the signal to noise ratio. It could be observed in Figure 1b that the echoes generated in the bone portion were much larger than those generated in the AC tissues. To effectively collect the ultrasound echoes scattered from the tissues inside the AC layer, which was relatively uniform in terms of ultrasound scattering in comparison with other tissues like muscles, the bone layer could not be too thick. However, too thin a layer of bone would affect the in situ behavior of the tissue, and would be bended into the hole during compression resulting complicated boundary conditions for the data analysis. The thickness of the bone layer used in this study was approximately 0.1~0.2 mm. Since the main solid matrix of AC is the collagen network, it was believed that the ultrasound echoes of the AC tissues were mainly scattered from the bundles of the collagen fibrils. Many recent investigations have targeted to establish the relationships between the acoustic parameters and the AC tissue components (Modest 1989, Agemura et al. 1990, Myers et al. 1995, Saied et al. 1997, Cherin et al. 1998, 2001, Toyras et al. 1999, Suh et al. 2001, Joiner et al. 2001, Nieminen et al. 2002). In those studies, the ultrasound beam was transmitted into the AC tissues via its articulating surface.

It was observed in this study that there was a region in the ultrasound echo train showing a different signal pattern in comparison with those of the bone and AC tissues, and its location corresponded to the calcified zone of AC as shown in Figure 1b. Similar patterns could be observed for most of the specimens. Another interesting observation was that the ultrasound echoes reflected from the cartilage-compressor interface possessed much lower frequency components in comparison with those generated in the AC tissues. It seemed that the porous compressor could absorb the high frequency components of the ultrasound wave.

In a previous study (Zheng et al. 2001), a contact 50 MHz ultrasound transducer with a silica delay line at the tip was used as a compressor to test the trypsin-digested AC specimens. Distinct ultrasound reflection signals were obtained from the interface of the digested and undigested portions of the AC specimens. One important criterion for the success of that method was the presence of a distinct front of degeneration, with significantly different acoustic properties before and after the front. In the present study, a focused ultrasound transducer was used instead, the ultrasound beam could be concentrated on a small area, and the tissues inside the AC could be better resolved. However, the bone layer used in this study severely attenuated the ultrasound signal. If a rigid material with an acoustic impedance similar to water and AC can be found, the AC specimen can be compressed on its articulating surface by this material. The focused ultrasound beam can pass though it, and strong ultrasound echoes from the AC can be collected for analysis. However, such an experimental setup may limit the selection of compressors, as porous compressors could not be used to load on the articulating surface of the cartilage. Porous compressors have been commonly used in the biomechanical assessment of AC in both confined and indentation configurations (Mow et al. 1980, 1991, Mak et al. 1987).

4.3 Resolutions

The movement of ultrasound signals under compression was determined using a cross-correlation tracking method in this study. The resolution of the displacement measurement depends on the sampling rate of an A/D converter. For an average ultrasound speed of 1660 m/s (Joiner et al. 2001), the theoretical displacement resolution was 1.66 μm for a 500 MHz sampling rate. The resolution for the displacement measurement can be improved using data interpolation or other signal processing techniques (Ophir et al. 1999, Bai et al. 1999). However, the artifacts of the processing need to be realized (Ophir et al. 1999). A/D converters with higher sampling rates and appropriate digital signal processing methods can also be used to further improve the displacement resolution of the measurement.

The axial resolution of the measurement, i.e. how fine sub-layers can be differentiated, depended on the frequency and the damping of ultrasound signals. For 35 MHz ultrasound, 2 cycles of damping period, and an ultrasound speed of 1660 m/s, the theoretical axial resolution of this method was approximately 50 μm (Bushong and Archer 1991), which was within the 0.2 mm interval of our ultrasound analysis. This resolution could be further improved by using higher frequency ultrasound. However, operating at higher frequencies would reduce the penetration depth of ultrasound waves in AC. The actual axial resolution also depended very much on the condition of the ultrasound signals scattered inside the AC layer. If the ultrasound echoes could not be detected in a certain region or vanished after compression, the deformation of the AC within this region could not be differentiated.

4.4 Boundary Conditions and Depth-dependent Deformation

Boundary conditions were important issues when interpreting the result of a compression test on AC. In this study, the specimens were tested in compression with a porous compressor used to press on its articulating surface. The interstitial fluid of the AC was allowed to leak through the lateral sides as well as the AC surface. Thus, a short relaxation time for reaching a state of equilibrium could be achieved. The testing system introduced in this study could readily be reconfigured for confined tests as well as indentation tests on the AC using both porous and impermeable compressors. The AC specimens used in this study comprised not only the full AC layer but also a thin layer of bone. In addition to keep the structural integrity of the AC to render the test as in-situ as possible, the bone layer could minimize the mechanical influence caused by the small hole under the specimen. The bone layer could prevent the AC from being squeezed into the hole during compression. Ultrasound-compression systems with confined and indentation configurations are also being used for the assessment of the depth-dependent properties of AC tissues in our lab.

It was demonstrated in this study that the axial strain distribution of the AC under compression was highly depth-dependent. The superficial layer incurred most of the

deformation applied on the AC. This profile of the strain distribution of AC in compression is due to the spatial variations of the water content, the proteoglycan concentration, and the orientation of the collagen fibrils (Mow et al. 1991). However, the nonuniformity of strain distribution observed in this study was more severe than that obtained previously using an optical microscopic method (Schinagl et al. 1996, 1997). The strains in the middle zone decreased gradually down to the deep zone in Schinagl's study. In the current study, the strains were rather small in the middle zone. However, detailed quantitative comparison between the results of Schinagl's study and ours is difficult because of the difference in the boundary conditions involved and in the duration of the force-relaxation. In Schinagl's study, the AC specimen was tested in a confined condition, and the AC tissues could not move laterally. While, the AC tissues could move laterally in the current study, as an unconfined setup was used. Another possible reason for this difference was that the AC specimens used in the two studies might be harvested from different locations. Since the loading patterns are different for the AC tissues at different locations of the joint, it could be expected that the pattern of the depth-dependent material properties might be different resulting different patterns of strain distribution under compression. This issue could be clarified in the future by testing AC tissues from different locations. In addition, the use of a simple saline bath solution in this study, rather than a phosphate-buffered saline (PBS) solution (PBS) with enzyme inhibitors used in Schinagl's study, might lead to some breakdown of AC matrix components resulting the change of the strain profile. Furthermore, a much longer force-relaxation time was adopted in Schinagl's study in comparison with the current study. As observed in Figure 4, the stress was not totally relaxed at the time when an equilibrium state was assumed. The results of this study might be complicated by the incomplete relaxation and by the residual interstitial fluid movement within an inhomogeneous medium. A longer relaxation time and even transient measurement in the future might clarify these issues.

4.6 Transient and dynamic measurement

The ultrasound-compression testing system introduced in this study will also be suitable for dynamic studies of AC with different compression rates, though only equilibrium depth-dependent strains were reported in this paper. As shown in Figure 6, the tissues at different depths inside the AC layers could still move in the force-relaxation phase after the ramp-compression was completed. This phenomenon has been predicted by biphasic theories of AC (Mow et al. 1980), but lacks of experimental evidences. It was demonstrated that the ultrasound-compression device reported in this study could be used to the transient behavior of the depth-dependent strains of AC specimens under compression, though the ultrasound echo trains were collected in a relative slow rate in this study (approximately 1 echo train per 10 seconds). The system is currently being improved to achieve a higher sampling rate. The transient responses of AC at different depths during compression and relaxation are being investigated. The results of transient depth-dependent properties of AC will be reported in another paper.

Acknowledgement

Portions of the work were supported by the Research Grant Council of Hong Kong (PolyU21/96M) and the Postdoctoral Fellowship Scheme of The Hong Kong Polytechnic University.

References

Agemura DH, O'Brien WD, Olerud JE, Chun LE, and Eyre DE. Ultrasonic propagation properties of articular cartilage at 100 MHz. Journal of Acoustic Society of America 1990; 87: 1786-1791.

Bai J, Fan Y, Li X, and Li X. Tracing echo segment selection method for strain

reconstruction. Ultrasonics 1999; 37: 51-57.

Bushong SC and Archer BR. Diagnostic Ultrasound: Physics, Biology, and Instrumentation. New York: Mosby-Year Book, Inc, 1991.

Chen AC, Bae WC, Schinagl RM, and Sah RL. Depth- and strain-dependent mechanical and electromechanical properties of full-thickness bovine articular cartilage in confined compression. Journal of Biomechanics 2001; 34: 1-12.

Cherin E, Saied A, Laugier P, Netter P, and Berger G. Evaluation of acoustical parameter sensitivity to age-related and osteoarthritic changes in articular cartilage using 50 MHz ultrasound. Ultrasound in Medicine and Biology 1998; 24: 341-354.

Cherin E, Saied A, Pellaumail B, Loeuille D, Laugier P, Gillet P, Netter P, and Berger G. Assessment of rat articular cartilage maturation using 50 MHz quantitative ultrasonography. Osteoarthritis and Cartilage 2001; 9: 178-186.

Cohn NA, Emelianov SY, Lubinski MA, and O'Donnell M. An elasticity microscope. Part I: Methods. IEEE Transactions on Ultrasonics, Ferroelectrics, and Frequency Control 1997a; 44: 1304-1319.

Cohn NA, Emelianov SY, and O'Donnell M. An elasticity microscope. Part II: Experimental Results, IEEE Transactions on Ultrasonics, Ferroelectrics, and Frequency Control 1997b; 44: 1320-1331.

Drogendijk AJ and Mow VC. Mapping of composition and biphasic material properties of cartilage over the patello-femoral grove. Trans 25th Annual Meeting of ORS 1982; 4: 142.

Fortin M, Buschmann MD, Bertrand MJ, Foster FS, and Ophir J. Cross-correlation of

ultrasound A-line to obtain dynamic displacement profiles within poroelastic materials undergoing stress-relaxation. Proc of SPIE on Medical Imaging 2000: Ultrasonic Imaging and Signal Processing; 3982: 286-294.

Guilak F, Ratcliffe A, Lane N, Rosenwasser MP, and Mow VC. Mechanical and biochemical changes in the superficial zone of articular cartilage in canine experimental osteoarthritis. Journal of Orthopaedic Research 1994; 12: 474-484.

Guilak F, Ratcliffe A, Mow VC. Chondrocyte deformation and local tissue strain in AC: A confocal microscopy study. Journal of Orthopaedic Research 1995; 12: 410-422.

Joiner GA, Bogoch ER, Pritzker KP, Buschmann MD, Chevrier A, and Foster FS. High frequency acoustic parameters of human and bovine articular cartilage following experimentally-induced matrix degradation. Ultrasonic Imaging 2001; 23: 106-116.

Kempson GE. The mechanical properties of articular cartilage. In: Sokoloff L, ed. The Joints and Synovial Fluid, vol. II. New York: Academic Press, 1980: 177-238.

Konofagou EE, Harrigan TP, Ophir J, and Krouskop TA. Poroelastography: imaging the poroelastic properties of tissues. Ultrasound in Medicine and Biology 2001; 27: 1387- 1397. Korhonen RK, Wong M, Arokoski J, Lindgren R, Helminen HJ, Hunziker EN, and Jurvelin JS. Importance of the superficial tissue layer for the indentation stiffness of articular cartilage. Medical Engineering and Physics 2002; 24: 99-108.

Mak AFT, Lai WM, and Mow VC. Biphasic indentation of articular cartilage: Part I theoretical analysis. Journal of Biomechanics 1987; 20: 703-714.

Mankin HJ, Mow VC, Buckwalter JA, Iannotti JP, and Ratcliffe A. Form and function of articular cartilage. In: Simnon SR, ed. Orthopaedic Basic Science. American

Academy of Orthopaedic Surgeons, 1994.

Mann RW, Shepherd DET, and Seedhom BB. Discussion on: A technique for measuring the compressive modulus of articular cartilage under physiological loading rates with preliminary results. Proc Instn Mech Engrs: J Engr Medicine 1999; 213 (H3): 291-292.

Mann RW, Shepherd DET, and Seedhom BB. Discussion on: A technique for measuring the compressive modulus of articular cartilage under physiological loading rates with preliminary results. Proc Instn Mech Engrs: J Engr Medicine 2001, 215 (H1): 123-124.

Modest VE, Murphy MC, and Mann RW. Optical verification of a technique for *in situ* ultrasonic measurement of articular cartilage thickness. Journal of Biomechanics 1989; 22: 171-176.

Mow VC, Kuei SC, Lai WM, and Armstrong CG. Biphasic creep and stress relaxation of articular cartilage in compression: Theory and experiment. J Biomech Engr 1980; 102: 73-84.

Mow VC, Zhu W, and Ratcliffe A. Structure and function of articular cartilage and meniscus. In: Mow VC, and Hayes WC, ed. Basic Othopaedic Biomechanics. New York: Raven Press, 1991: 143-198.

Myers SL, Dines K, Brandt DA, Brandt KD, and Alvrecht ME. Experimental assessment by high frequency ultrasound of articular cartilage thickness and osteoarthritic changes. Journal Rheumatology 1995; 22: 109-116.

Nieminen HJ, Toyras J, Rieppo J, and Nieminen MT. Real-time ultrasound analysis of

articular cartilage degradation in vitro. Ultrasound in Medicine and Biology 2002; 28: 519-525.

Ophir J, Cespedes I, Ponnekanti H, Yazdi Y, and Li X. Elastography: a quantitative method for imaging the elasticity of biological tissues. Ultrasonic Imaging 1991; 13: 111-134.

Ophir J, Alam SK, Garra B, Kallel F, Konofagou E, Krouskop T, and Varghese T. Elastography: ultrasonic estimation and imaging of the elastic properties of tissues. Proc Instn Mech Engrs 1999; 213 (Part H): 203-233.

Qin L, Zheng YP, Leung CT, Mak AFT, Choy WY, and Chan KM. Ultrasound detection of trypsin-treated articular cartilage – Its association with cartilaginous proteoglycans assessed by histological and biochemical methods. Journal of Bone Mineral and Metabolism. In press, 2002.

Roth V, and Mow VC. The intrinsic tensile behavior of the matrix of bovine articular cartilage and its variation with age. Journal of Bone and Joint Surgery 1980; 62A: 1102-1117.

Saied A, Cherin E, Gaucher H, Laugier P, Gillet P, Floquet J, Netter P, and Berger G. Assessment of articular cartilage and subchondral bone: subtle and progressive changes in experimental osteoarthritis using 50MHz echography in vitro. Journal of Bone and Mineral Research 1997; 12: 1378-1386.

Schinagl RM, Ting MK, Price JH, and Sah RL. Video microscopy to quantitate the inhomogeneous equilibrium strain within articular cartilage during confined compression. Annals of Biomedical Engineering 1996; 24: 500-512.

Schinagl RM, Gurskis D, Chen AC, and Sah RL. Depth-dependent confined compression modulus of full-thickness bovine articular cartilage. Journal of Orthopaedic Research 1997; 15: 499-506.

Setton LA, Zhu W, and Mow VC. The biphasic poroviscoelastic behavior of articular cartilage: Role of the surface zone in governing the compressive behavior. Journal of Biomechanics 1993; 26: 581-592.

Suh JKF, Youn I, and Fu FH. An in situ calibration of an ultrasound transducer: a potential application for an ultrasonic indentation test of articular cartilage. Journal of Biomechanics 2001; 34: 1347-1353.

Toyras J, Rieppo J, Nieminen MT, Helminen HJ, and Jurvelin JS. Characterization of enzymatically induced degradation of articular cartilage using high frequency ultrasound. Physics in Medicine and Biology 1999; 44: 2723-2733.

Wang CCB, Hung CT, and Mow VC. An analysis of the effects of depth-dependent aggregate modulus on articular cartilage stress-relaxation behavior in compression. Journal of Biomechanics 2001; 34: 75-84.

Woo SLY, Akeson WH, and Jemmott GF. Measurements of nonhomogeneous, directional mechanical properties of articular cartilage in tension. Journal of Biomechanics 1976; 9: 785

Zheng YP and Mak AFT. An ultrasound indentation system for biomechanical properties assessment of soft tissues *in vivo.* IEEE Transactions on Biomedical Engineering 1996; 43: 912-918.

Zheng YP, Mak AFT, Qin L, and Ding CX. Ultrasound elastography of articular

cartilage: A preliminary study. Proc 20th Annual International Conference of IEEE EMBS, Hong Kong, 1998: 1940-1942.

Zheng YP and MaK AFT. Effective elastic properties for lower limb soft tissues from manual indentation experiment. IEEE Transactions on Rehabilitation Engineering 1999a; 7: 257-267.

Zheng YP, Mak AFT. Extraction of quasilinear viscoelastic parameters for lower limb soft tissues from manual indentation experiment. ASME Transactions, Journal of Biomechanical Engineering 1999b; 121: 330-339.

Zheng YP, Ding CX, Bai J, and Mak AFT. Measurement of nonhomogeneous compressive properties of trypsin treated articular cartilage: An ultrasound investigation. Medical and Biological Engineering and Computing 2001; 39: 534-541.

Figure Captions

Figure 1. (a) A typical histological image of the central portion of an AC specimen stained with Safranin-O (Proteoglycan was stained in red in a color image). White triangles indicate the AC surface and blank ones indicate the AC-bone interface, which was a regions of calcified AC. (b) Ultrasound echo signals generated by a cartilage specimens. It was used to indicate where the corresponding echoes were generated, though the specimen was not the same as that shown in (a).

Figure 2. The ultrasound-compression system for the study of articular cartilage. **(A)** Micrometer; **(B)** Moving bar; **(C)** Load cell; **(D)** Porous compressor; **(E)** AC specimen; **(F)** Specimen platform with a hole of Φ0.5mm at the center; **(G)** Chamber filled with saline solution; **(H)** 50 MHz focused ultrasound transducer.

Figure 3. The actual movement of the AC surface as detected by ultrasound when a compression rate of approximately 0.2 mm/min was attempted manually. The mean and standard deviation were calculated using the results of the 10 tests for different specimens.

Figure 4. A typical two-step compression and stress relaxation procedure used in this study.

Figure 5. A typical set of ultrasound signals of an AC specimen. **(a)** Echoes obtained after 0.1mm pre-compression; **(b)** Echoes obtained after the first 0.1mm compression and relaxation; **(c)** Echoes obtained after the second 0.1mm compression and relaxation. The ultrasound signals of the bone portions as shown in Figure 1(b) was removed to highlight the signals of the cartilage portions which was relatively weak.

Figure 6. The depth-dependent displacements of tissues of a typical AC specimen at different time points. The displacements of different tissue layers were measured by

cross-correlation tracking for the corresponding ultrasound echoes. The equilibrium strains was calculated using the data at the time of 400 s.

Figure 7. (a), (c) and (e) Depth dependent displacements after the first compression of the cartilage specimen #1, #3, and #8, respectively. (b), (d) and (f) Depth dependent displacement after the second compression of the three corresponding specimens. The two curves in each figure indicate the results of two different tests with the same approach but with a time interval of at least 2 hours. Square and circle marks represent the results of the first and second measurement, respectively.

Figure 8. The mean equilibrium strains of sub-layers at different depths after two incremental compressions and subsequent relaxations were applied. The error bars represent the standard deviations of the results of 10 specimens.

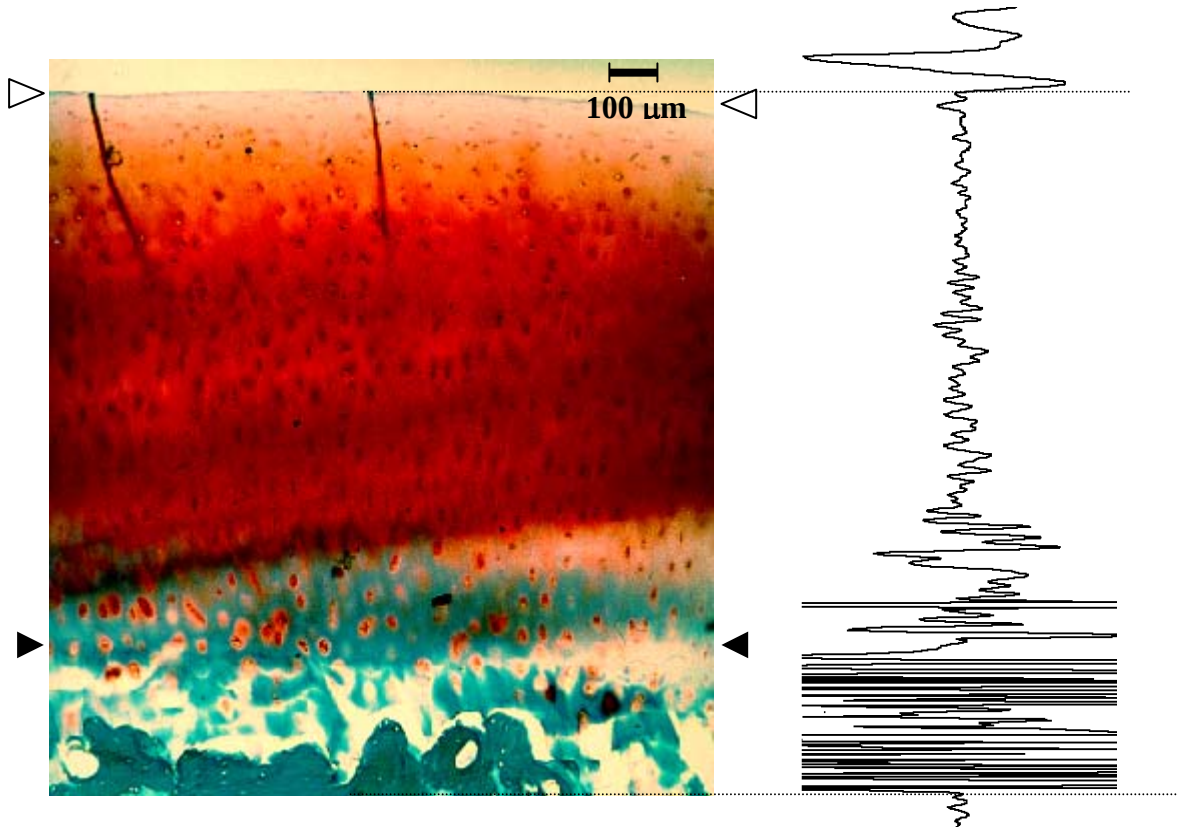

Figure 1

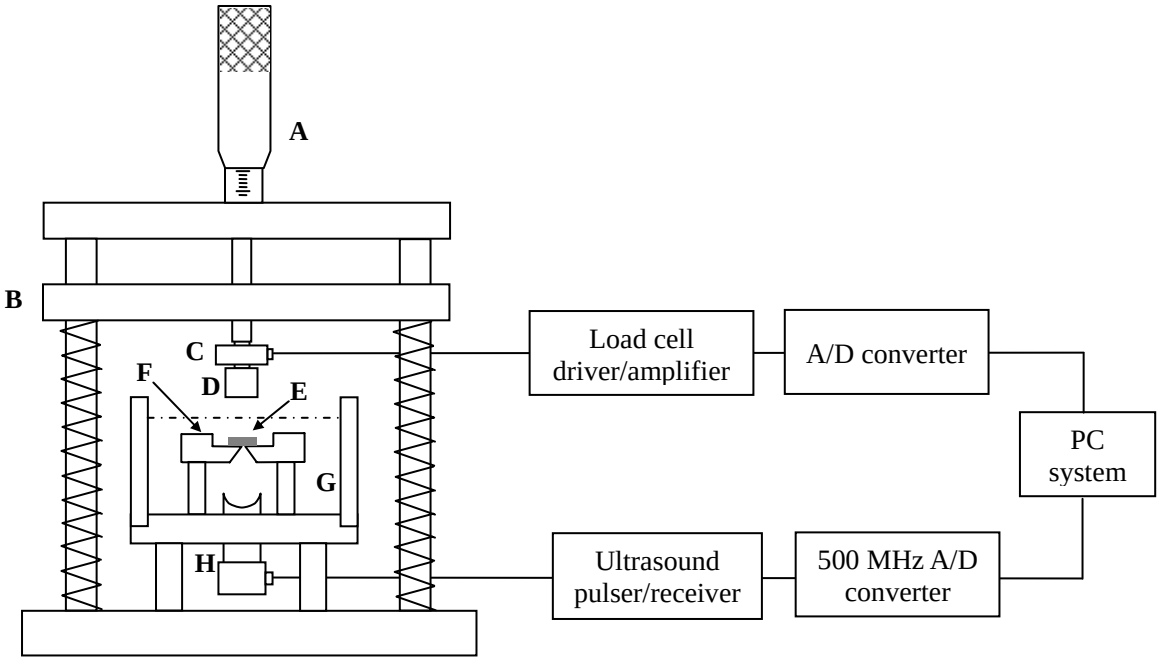
A
B
C
F
D
E
G
H
Load cell driver/amplifier
A/D converter
PC system
Ultrasound pulser/receiver
500 MHz A/D converter

Figure 2

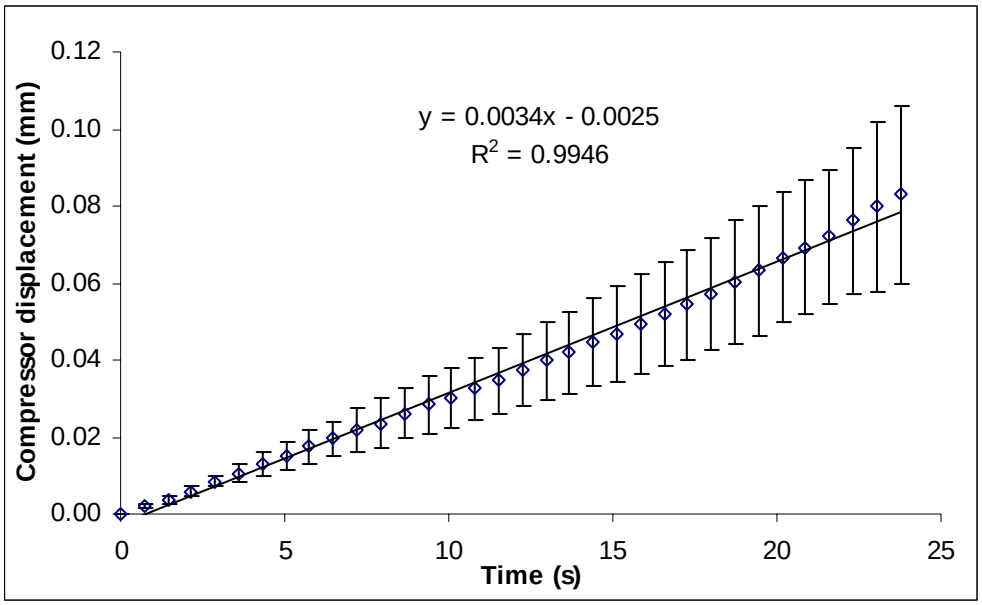
0.12
0.10
0.08
0.06
0.04
0.02
0.00
Compressor displacement (mm)
y = 0.0034x - 0.0025
R2 = 0.9946
0
5
10
15
20
25
Time (s)

Figure 3

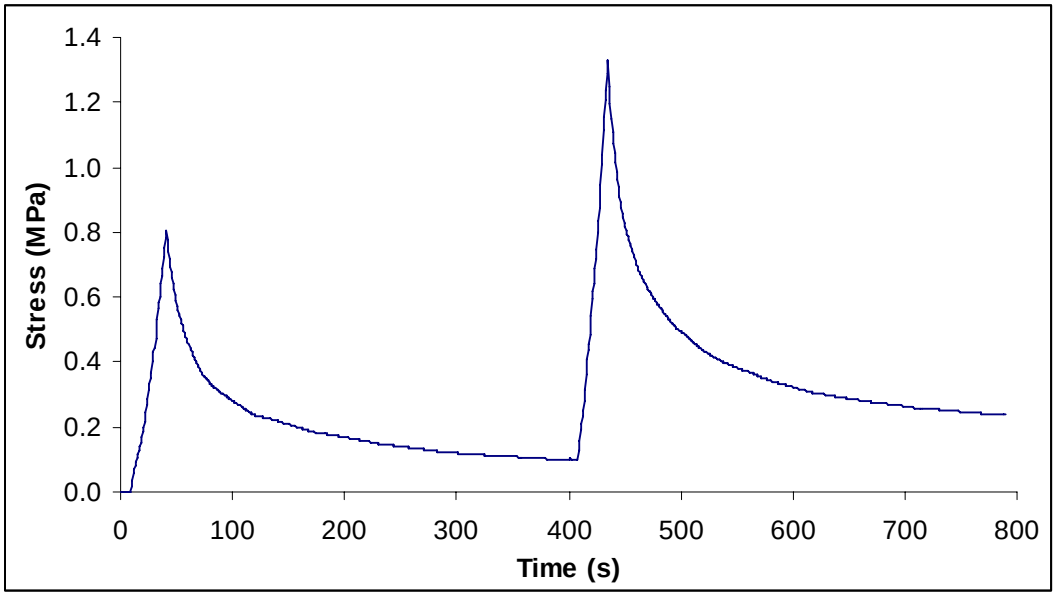
1.4
1.2
1.0
0.8
0.6
0.4
0.2
0.0
Stress (MPa)
0
100
200
300
400
500
600
700
800
Time (s)

Figure 4

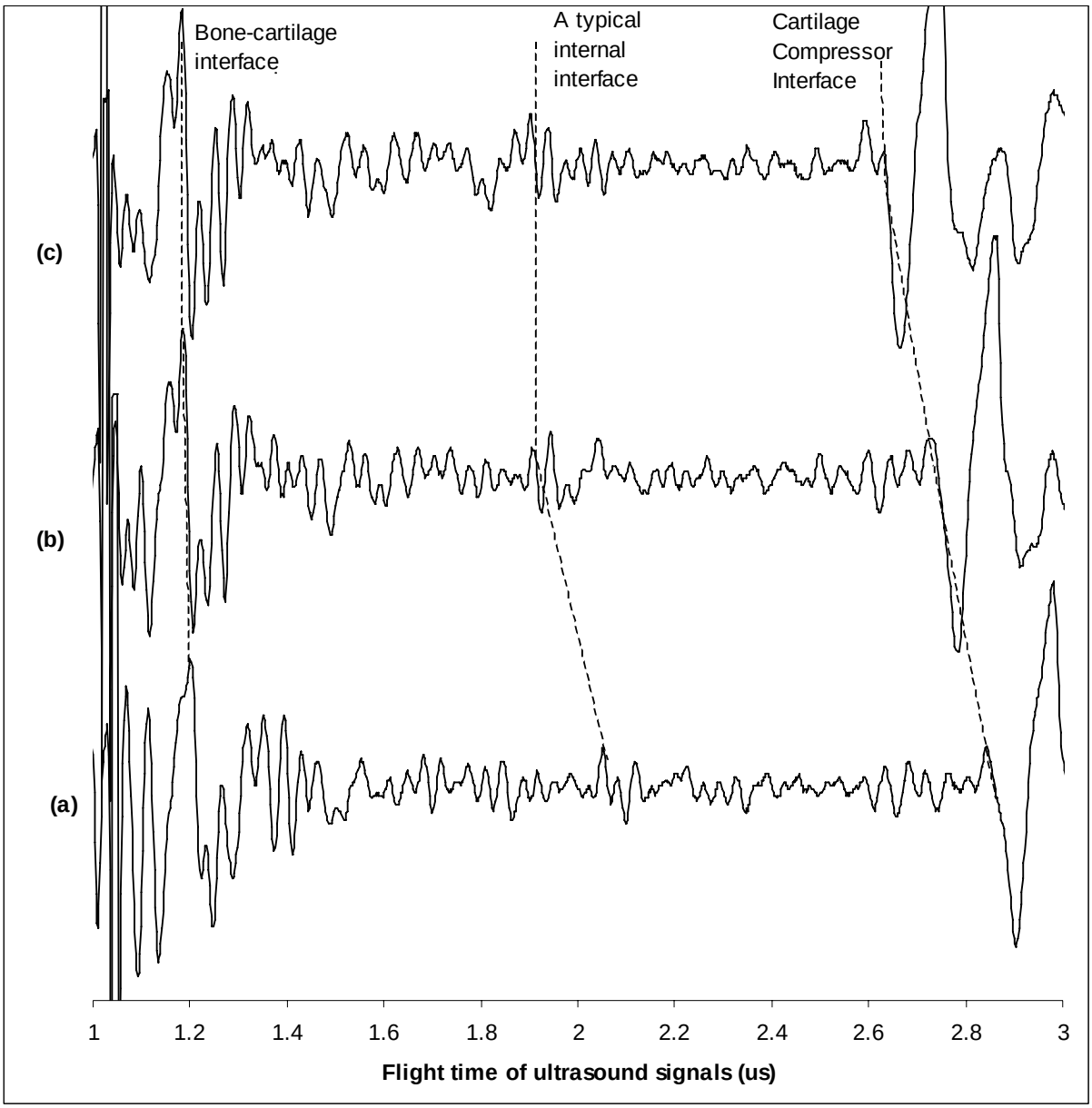
Bone-cartilage interface
A typical internal interface
Cartilage Compressor Interface
(c)
(b)
(a)
1
1.2
1.4
1.6
1.8
2
2.2
2.4
2.6
2.8
3
Flight time of ultrasound signals (us)

Figure 5

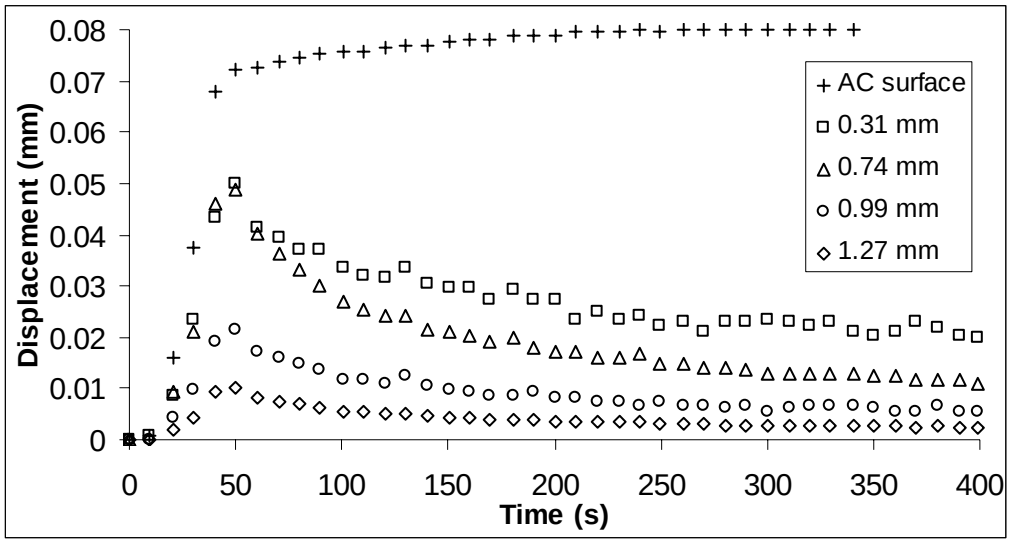
Displacement (mm)
0.08
0.07
0.06
0.05
0.04
0.03
0.02
0.01
0
0
50
100
150
200
250
300
350
400
Time (s)
AC surface
0.31 mm
0.74 mm
0.99 mm
1.27 mm

Figure 6

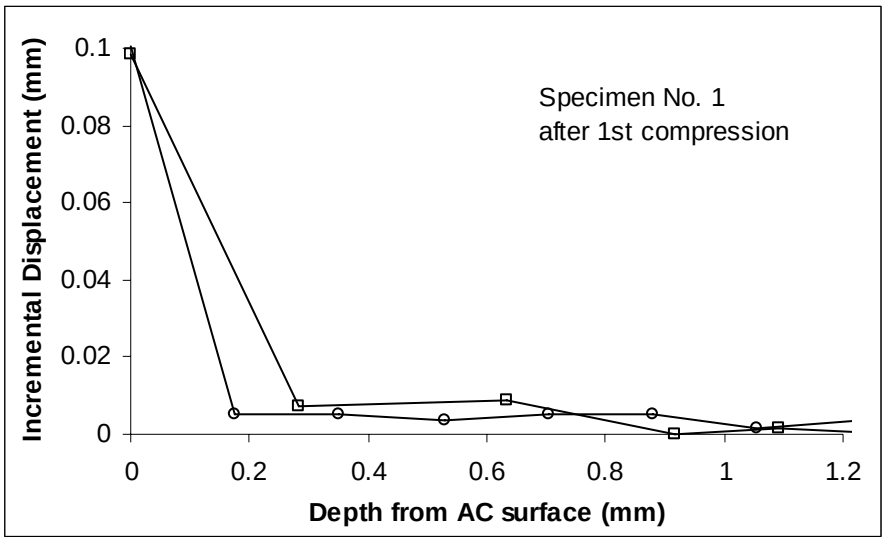

Figure 7 (a)

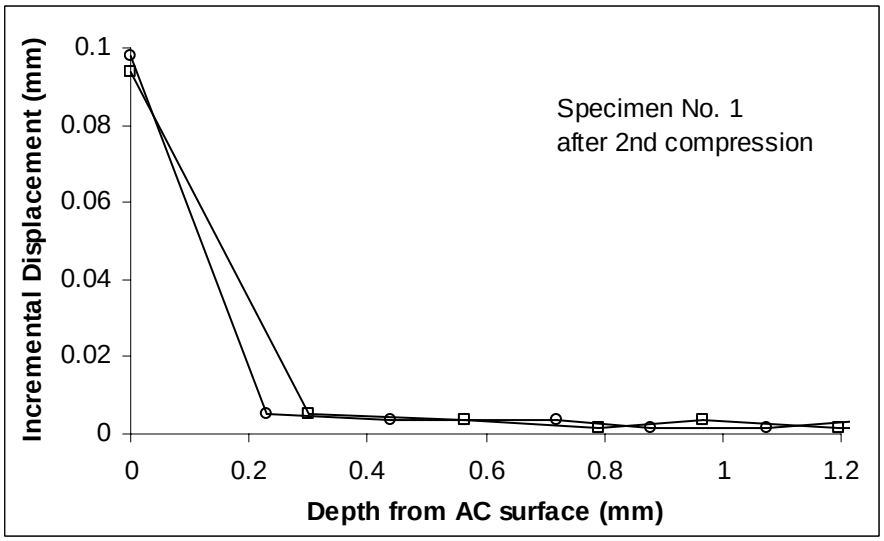

Figure 7 (b)

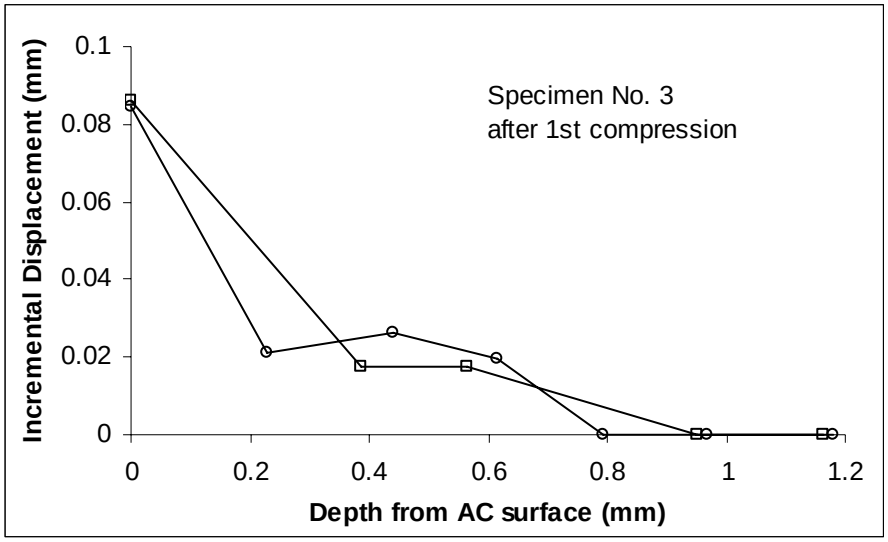

Figure 7 (c)

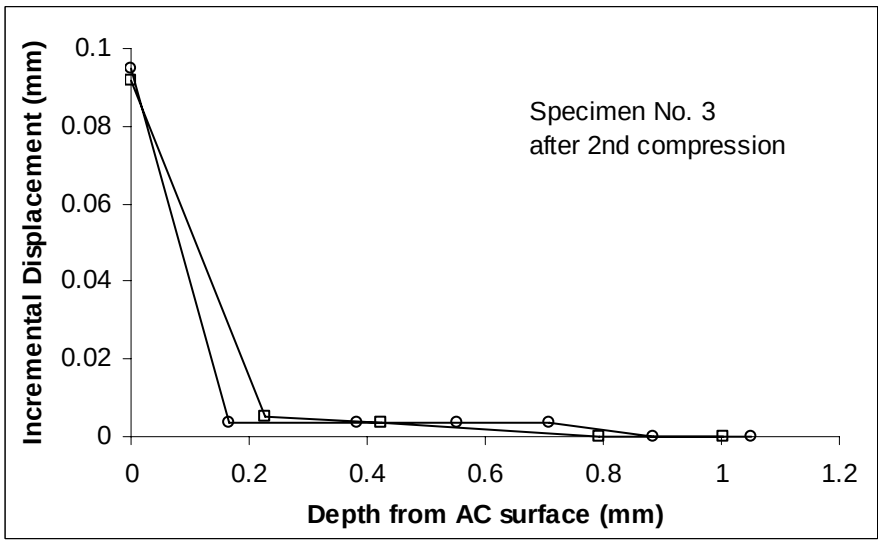

Figure 7 (d)

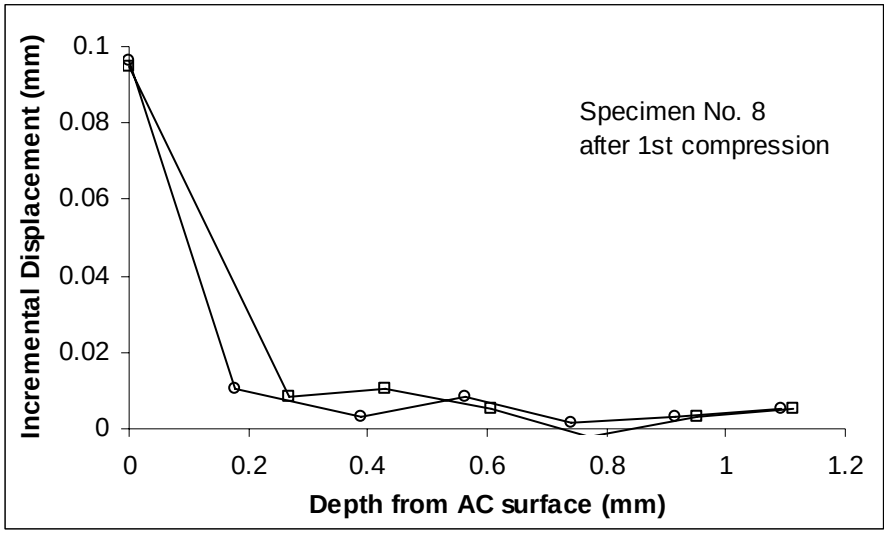

Figure 7 (e)

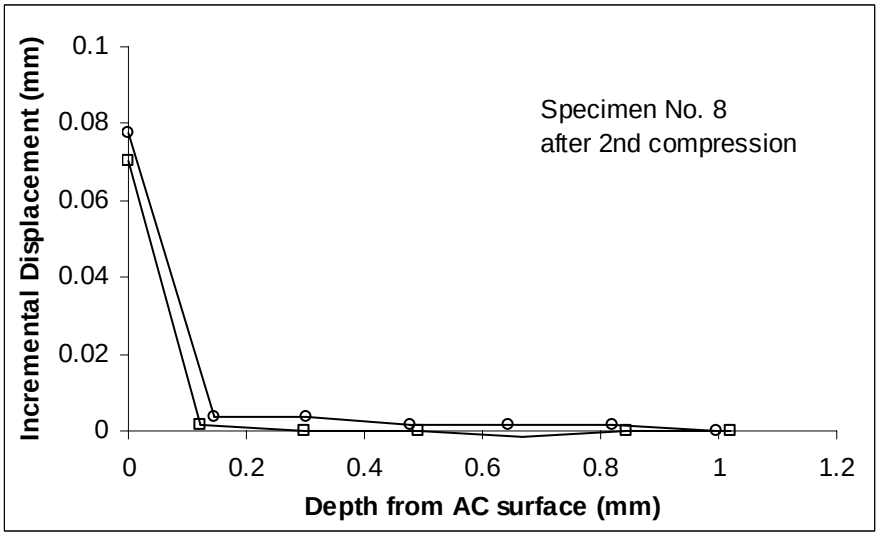

Figure 7 (f)

Figure 7

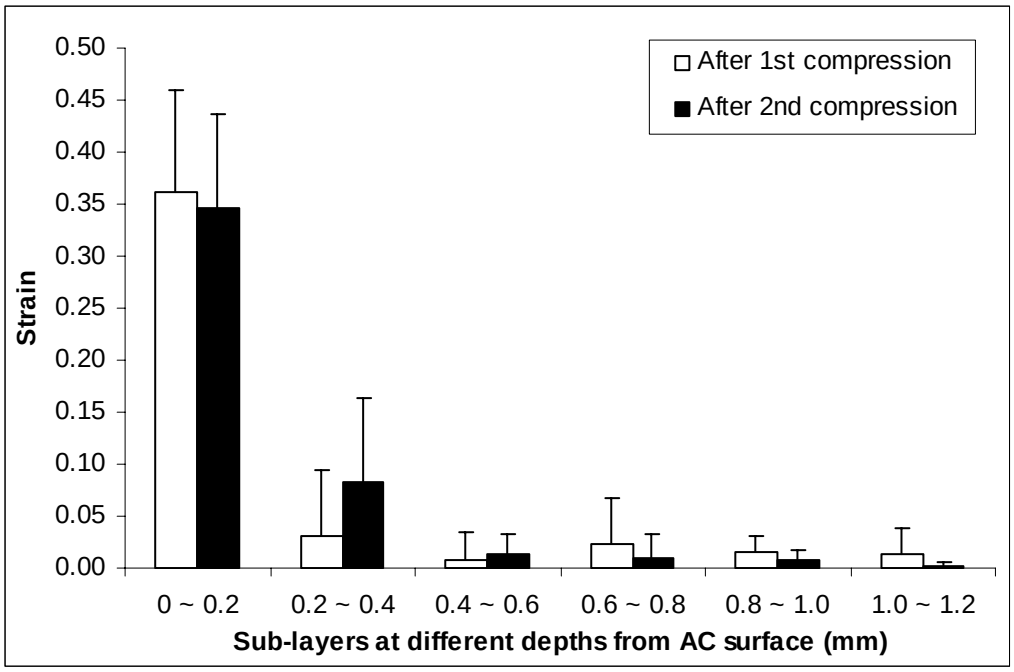
0.50
0.45
0.40
0.35
0.30
0.25
0.20
0.15
0.10
0.05
0.00
Strain
After 1st compression
After 2nd compression
0 ~ 0.2
0.2 ~ 0.4
0.4 ~ 0.6
0.6 ~ 0.8
0.8 ~ 1.0
1.0 ~ 1.2
Sub-layers at different depths from AC surface (mm)

Figure 8